NIH Public Access
Author Manuscript
J Med Chem. Author manuscript; available in PMC 2014 June 16.

Published in final edited form as:
J Med Chem. 2013 May 9; 56(9): 3467–3477. doi:10.1021/jm400351a.

Identification of Selective and Potent Inhibitors of Fibroblast Activation Protein and Prolyl Oligopeptidase

Sarah E. Poplawski[†,‡], **Jack H. Lai**[†,‡], **Youhua Li**[†], **Zhiping Jin**[†], **Yuxin Liu**[†], **Wengen Wu**[†], **Yong Wu**[†], **Yuhong Zhou**[†], **James L. Sudmeier**[†], **David G. Sanford**[†,‡], and **William W. Bachovchin**[*,†,‡]

[†]Department of Biochemistry, Tufts University Sackler School of Biomedical Sciences, 136 Harrison Avenue, Boston, Massachusetts 02111, United States

[‡]Arisaph Pharmaceuticals, Inc., 100 High Street, Suite 1202, Boston, Massachusetts 02110, United States

Abstract

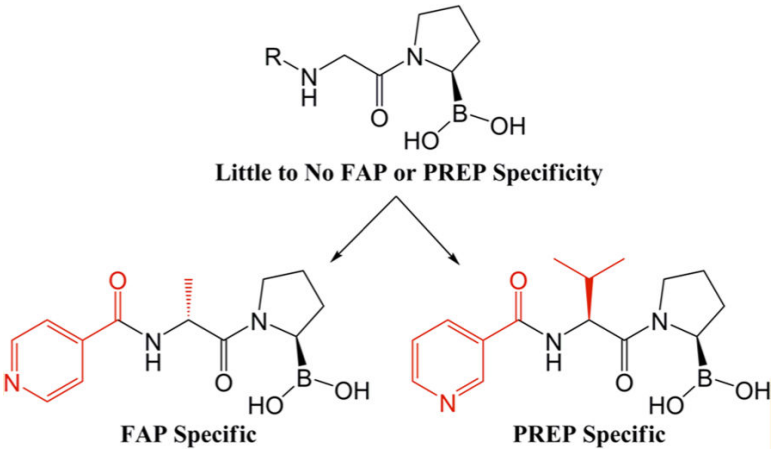

Fibroblast activation protein (FAP) is a serine protease selectively expressed on reactive stromal fibroblasts of epithelial carcinomas. It is widely believed to play a role in tumor invasion and metastasis and therefore to represent a potential new drug target for cancer. Investigation into its biological function, however, has been hampered by the current unavailability of selective inhibitors. The challenge has been in identifying inhibitors that are selective for FAP over both the dipeptidyl peptidases (DPPs), with which it shares exopeptidase specificity, and prolyl oligopeptidase (PREP), with which it shares endopeptidase specificity. Here, we report the first potent FAP inhibitor with selectivity over both the DPPs and PREP, *N*-(pyridine-4-carbonyl)-D-Ala-boroPro (ARI-3099, **6**). We also report a similarly potent and selective PREP inhibitor, *N*-(pyridine-3-carbonyl)-Val-boroPro (ARI-3531, **22**). Both are boronic acid based inhibitors, demonstrating that high selectivity can be achieved using this electrophile. The inhibitors are

© 2013 American Chemical Society

[*]**Corresponding Author**: Phone: 617-636-6881. william.bachovchin@tufts.edu. .

Notes
The authors declare no competing financial interest.

Johns Hopkins University EX2020
GE Healthcare v. Johns Hopkins
PGR2025-00059

NIH-PA Author Manuscript
NIH-PA Author Manuscript
NIH-PA Author Manuscript

NIH-PA Author Manuscript

NIH-PA Author Manuscript

NIH-PA Author Manuscript

stable, easy to synthesize, and should prove to be useful in helping to elucidate the biological functions of these two unique and interesting enzymes, as well as their potential as drug targets.

INTRODUCTION

Fibroblast activation protein (FAP) is a type II, membrane-bound serine protease highly expressed on activated stromal fibroblasts of essentially all epithelial cell carcinomas but not on the cancer cells themselves, normal fibroblasts, or normal tissues.[1–4] FAP is most closely related to dipeptidyl peptidase IV (DPPIV, EC 3.4.14.5), with which it shares 54% sequence homology, membership in protease clan SC subfamily S9B, and the relatively rare ability to cleave peptides after proline residues. Other human enzymes with post-proline cleaving activity include dipeptidyl peptidase 8 (DPP8), dipeptidyl peptidase 9 (DPP9), dipeptidyl peptidase II (DPPII, EC 3.4.14.2), and prolyl oligopeptidase (PREP, EC 3.4.21.26).[5–7] The dipeptidyl peptidases (DPPs) are exclusively exopeptidases, whereas PREP is exclusively an endopeptidase. FAP is unique in having both exo- and endopeptidase activities.[4,8]

Post-proline cleaving enzymes are expected to have important biological functions in part because of the unique structure of proline but also because many bioactive peptides contain conserved proline residues at sites that appear to serve as key recognition elements for proteolytic processing.[9] Of the human post-proline cleaving enzymes, only the biological function of DPPIV has thus far been discovered and described. DPPIV regulates the incretin hormones glucagon-like peptide 1 (GLP-1) and glucose-dependent insulinotropic peptide (GIP) and, as a result, is now a validated target for the treatment of type 2 diabetes.[10–12]

The unique expression profile of FAP, coupled with studies indicating that it plays an important role in supporting tumor growth and metastasis, has generated interest in FAP as a therapeutic target.[13–15] Tumors have been reported to grow more slowly in FAP knockout mice and more rapidly when transfected with FAP.[16,17] Kramen et al. have reported that genetic depletion of FAP-positive fibroblasts in a mouse lung cancer model results in hypoxic necrosis of tumor and stromal cells via elicitation of an immune response mediated by TNF-α and IFN-γ.[18] This is especially exciting, as it indicates that FAP may promote tumor growth, at least in part, by helping to hold the host's antitumor immune response at bay and therefore suggests that FAP targeted therapies may help to turn on antitumor immunity. The mechanisms through which FAP mediates the above effects, however, are essentially unknown. It is not even clear whether or not its protease activity is involved, although inhibitors have been reported to have antitumor effects, including those mediated via enhancement of antitumor immunity.[19,20] The inhibitors used in these experiments were not entirely specific for FAP, however, usually cross-reacting with the DPPs, PREP, or both, rendering the connection between the protease activity and tumor growth promoting activities of FAP less than certain.

The current lack of specific FAP inhibitors is therefore an important factor hampering investigation of FAP's biological functions and its potential as a new target for anticancer drugs. The problem stems from FAP's dual function as both an exo- and endopeptidase. Identifying inhibitors that are specific for FAP over the DPPs, or for FAP over PREP, is

NIH-PA Author Manuscript

NIH-PA Author Manuscript

NIH-PA Author Manuscript

relatively simple, and such inhibitors exist.[21,22] Identifying inhibitors that are specific for FAP over both the DPPs and PREP at the same time is more difficult.

Tsai et al. have reported that several substituted 4-carboxymethylpyroglutamic acid diamides are selective inhibitors of FAP.[23] While they screened these compounds against several of the DPPs, they did not screen against PREP, so it is not clear whether or not these inhibitors are truly specific and to what degree. Ryabtsova et al. described the design of a series of acylated Gly-(2-cyano)pyrrolidines to specifically address FAP selectivity versus PREP.[24] The bulk of the inhibitors described were not particularly potent, however, and they ultimately concluded that "selectivity toward the endopeptidase PREP was found to be less evident" in comparison to the other dipeptidyl peptidases. Thus, no FAP inhibitors thus far claimed to be specific for FAP have been demonstrated to be selective over PREP. PREP, like DPPIV and FAP, belongs to protease clan SC but to a different subfamily, S9A. Also similar to FAP, it has both soluble and membrane-bound forms, although the soluble form of PREP is generally localized the cytosol, whereas the soluble form of FAP is in the plasma.[25,26] PREP is highly conserved in mammals and widely distributed in cells and tissues, with especially high concentrations found in the brain.[27,28]

Small molecule inhibitors of serine proteases are often divided into two categories, covalent and noncovalent. Covalent inhibitors are those that incorporate functional groups designed to be attacked by, and to form a covalent bond with, the active site serine. Such functional groups have been called transition-state analogues, serine traps, or electrophiles. Covalent inhibitors can be reversible or irreversible. Examples of reversible covalent inhibitors include those incorporating aldehyde, nitrile, boronic acid, or α-ketoamide functional groups. Examples of irreversible covalent inhibitors include those incorporating chloromethyl ketone, phosphoro–fluoridate, or phosphonate ester groups. At the present time, conventional wisdom still appears to strongly prefer non–covalent over covalent inhibitors, whether reversible or not, for use as drugs.[29] There are several reasons for this, but the most important is a belief that covalent inhibitors are too reactive to yield inhibitors specific enough to be safe for use in humans.[30,31] Thus, statements can be found in the literature prior to 2000 to the effect that covalent inhibitors, including those incorporating any of the electrophiles mentioned above would be too reactive to be sufficiently specific to ever yield a marketed drug.[32] As of 2011, however, there are at least 39 examples of covalent inhibitors approved by the FDA. Of the 15 drugs on the market that target serine or threonine proteases, seven, or nearly half, contain an electrophile. These include one boronic acid, two α-ketoamides, and two nitriles.[33]

Here we report the design and characterization of boronic acid based inhibitors for FAP and PREP that combine low nanomolar potency with high selectivity. *N*-(Pyridine-4-carbonyl)-D-Ala-boroPro (ARI-3099, **6**) is more than 350-fold selective for FAP over PREP, with negligible potency against the DPPs, while *N*-(pyridine-3-carbonyl)-Val-boroPro (ARI-3531, 22) displays even greater selectivity for PREP over FAP (77 000-fold) while also not inhibiting the DPPs.

NIH-PA Author Manuscript

NIH-PA Author Manuscript

NIH-PA Author Manuscript

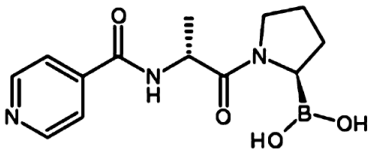

6

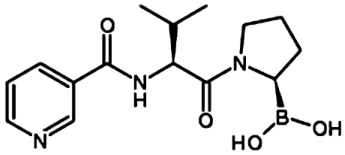

22

The fact that boronic acid-based compounds can discriminate between enzymes with specificities as closely overlapping as the post-proline cleaving enzymes demonstrates the high selectivity that can be achieved with this electrophile.

RESULTS AND DISCUSSION

P_1 and P_2 Substrate Specificity of FAP

Specificity profiling demonstrates that FAP, like all members of this family, strongly prefers cleaving after proline residues. This applies to both its exo- and endopeptidase activities (Figure 1, top). The P_2 specificity, however, is quite different for the exo- and endopeptidase activities (Figure 1, bottom). As an exopeptidase, FAP accepts essentially all residues at P_2 with proline, large, hydrophobic, aromatic, and positively charged residues preferred most and negatively charged side chains preferred least. As an endopeptidase, FAP exhibits an absolute requirement for glycine at P_2; no other naturally occurring amino acid is accepted. This agrees with previous FAP specificity studies and explains why many FAP inhibitors are based upon an X-Gly-Pro sequence.[21,34,35] While this structural motif confers specificity against DPPs, it generally does not prevent cross-reactivity with PREP.

Selective Inhibitors of FAP

A recent review cited Tran et al. as having reported that a nonpeptidic boroproline inhibitor, 1-(2-(1-oxoisoindolin-2-acetyl)-boroPro (**4**), is approximately 400-fold selective for FAP over PREP.[36] Tran et al. actually reported that **4** is only 3-fold selective for PREP over FAP,[22] a finding with which our results essentially agree (Table 1). Furthermore, Tran et al. reported that a P_2 D-alanine-containing inhibitor, N-acetyl-D-Ala-boroPro (**3**), exhibits modest potency (K_i of 350 nM) and specificity (7.7-fold) for FAP over PREP. Our results agree that **3** inhibits FAP with modest potency but disagree that it is selective for FAP over PREP; we find instead that 3 is modestly selective for PREP over FAP. Nevertheless, both results suggest that FAP is capable of tolerating a P_2 D-alanine in the context of an X-boroPro-based inhibitor.

Of the compounds reported here, Gly-boroPro (1) demonstrates the greatest degree of selectivity for FAP over PREP (900-fold). Because of the presence of the free N-terminal amino group, however, **1** exhibits essentially no selectivity for FAP over the DPPs. Addition of various N-terminal blocking groups to **1**, as shown with **2** and **5**, provides increased potency against FAP, elimination of cross-reactivity with the DPPs, but little to no selectivity for FAP over PREP. Replacement of the P_2 glycine of **5** with a D-alanine (**6**) provides 360-fold selectivity for FAP over PREP while retaining FAP potency in the low nanomolar range.

NIH-PA Author Manuscript

NIH-PA Author Manuscript

NIH-PA Author Manuscript

Optimization of the N-Terminal Blocking Group

A number of variations of the X-D-Ala-boroPro scaffold were assessed, with **6** possessing the most optimal combination of potency and selectivity. Both the presence of the nitrogen and its position in the pyridine ring proved to be important. The former provides selectivity for FAP, while the latter provides additional potency, as is evident in comparing **6** with **7** and **8** (Table 2). The nitrogen atom at the 4- or para position appears optimal. Without a solved structure of FAP complexed to **6**, we cannot be certain why this is the case. However, through molecular modeling beginning with the existing homologous X-ray crystal structure of the DPPIV tetrahedral intermediate complexed with diprotinA, as performed by previous researchers,[21,34] we discovered a reasonable hypothesis for the role of the pyridine group. Positioning the -boroPro moiety into the hydrophobic S_1 pocket of FAP in a manner consistent with the diprotinA structure, the P_2 D-alanyl and 4-pyridylcarbonyl groups are oriented for an optimal fit. The resulting model strongly suggests that a protonated pyridine nitrogen atom in the 4-position could form a hydrogen bond with the backbone carbonyl oxygen of Glu[204]. The pyridyl nitrogen should have a pK_a of approximately 5.5, so it would not be unreasonable for it to be protonated in the complex. PREP does not have a corresponding carbonyl oxygen or any other functional group that could act as a hydrogen bond acceptor in this position.

Addition of halo substituents (F and Cl) to the pyridine ring also appears to further improve potency against FAP but with a 2- to 3-fold loss in selectivity over PREP (**9**–**12**). There are several possible explanations for this. The electron withdrawing effect of fluorine and chlorine would be expected to reduce the pK_a of the pyridyl nitrogen, making it a stronger acid. Although this would reduce the fraction of protonated inhibitor in solution, it would make the pyridyl N–H a stronger hydrogen bond donor in the complex. Fluorine at this position enhances binding considerably less than chlorine, however, suggesting that the effect is more likely mediated by a steric or torsion angle change rather than an electronic effect. As torsion angle changes could have an effect on PREP binding as well, this may explain why these inhibitors are less selective for FAP over PREP in comparison to **6**.

Effects of P_2 D-Amino Acid Variation on FAP and PREP Inhibition

The finding that a D-alanine in P_2 provides significant selectivity for FAP over PREP prompted us to examine other D-amino acids in this position (Table 3). For this purpose we employed a dipeptide-boroPro scaffold with an *N*-(4-quinolinoyl) group substituted at the N-terminus. As before, placement of D-alanine at the P_2 position in this scaffold yields a potent and highly selective FAP inhibitor (**13**). Increasing the size of the D-amino acid at P_2 quickly leads to losses of both potency and FAP selectivity. In fact, the larger P_2 substitutions lead to such large and selective losses in potency toward FAP that the inhibitors become selective for PREP over FAP (**15**, **17**, **18**, and **19**).

Selective Inhibitors of PREP

Identifying potent and selective inhibitors for PREP is a far more simple task than for FAP. N-Terminal substitution provides, at once, selectivity for PREP over all of the DPPs and over the exopeptidase activity of FAP. The problem then reduces to discriminating between the endopeptidase activities of PREP and FAP, which is relatively straightforward, as FAP's

NIH-PA Author Manuscript

NIH-PA Author Manuscript

NIH-PA Author Manuscript

endopeptidase activity has rather stringent requirements at P_2, accepting so far only glycine or D-alanine, whereas PREP is more promiscuous and will accept a variety of amino acids at this position.[37] Thus, blocking the N-terminus of Val-boroPro (**20**), which exhibits little to no selectivity against any of the post-proline cleaving enzymes, produces 22, which combines 1 nM potency against PREP with greater than 77 000-fold selectivity over FAP, as well as the DPPs (Table 4). Substituting glycine for valine at P_2 in 22 produces a potent inhibitor (**21**) of both FAP and PREP, demonstrating that the P_2 valine provides selectivity for PREP over FAP.

Determination of Competitive or Noncompetitive Inhibition

Given the structural similarities of **6** and **22** to the substrates used for IC_{50} determinations, it was anticipated that they would be competitive inhibitors of FAP and PREP. This is in fact the case, as shown by the Lineweaver–Burk plots for **6** in Figure 2. This kinetic analysis also provided K_i values for these two inhibitors (Table 5). The K_i values of **6** against FAP and PREP are lower than the IC_{50} values, but the ratio of selectivity remains the same, as expected. As before, the selectivity of **22** for PREP over FAP could only be quantified as greater than 140 000-fold, as **22** does not inhibit FAP at the highest concentrations tested.

Inhibitor Selectivity in Vitro in Mock and mFAP Transfected Cells

Although **6** and **22** are here shown to be potent and selective inhibitors of FAP and PREP, one may question whether the selectivity can be demonstrated in a more biologically relevant milieu, such as in cell cultures. Therefore, HEK293 cells transfected with either murine FAP (mFAP) or a mock vector were incubated with 1 μM **2**, **6**, or **22**. Compound **2**, which is a relatively poor inhibitor of DPPIV, DPP8, and DPP9, but a potent inhibitor of both FAP and PREP, inhibited virtually all of the cellular prolyl endopeptidase activity in both cell lines (Figure 3). The PREP specific inhibitor **22** inhibited all activity in the mock-transfected cells but only approximately 60% in the mFAP transfected cells. This demonstrates that all of the endogenous prolyl endopeptidase activity in the HEK293 cells can be attributed to PREP, in agreement with previously published results that showed that HEK293 cells do not express endogenous FAP.[38] Finally, the FAP specific inhibitor **6** reduced activity only in the mFAP transfected cells but not in mock transfected cells. Not only do these findings demonstrate specificity in a cell-culture-based setting, they also indicate that **6** inhibits mouse and human FAP.

Effect of the Presence of PREP on the Selectivity of 6 toward FAP

Unlike the in vitro assays used to determine the previously reported IC_{50} values, the cellular-based assay in Figure 3, as well as any future in vivo assays, involves a mixture of enzymes rather than a single purified enzyme. The chief competitor for a FAP inhibitor in vivo will likely be PREP. Therefore, the effect of varying concentrations of PREP on FAP inhibition by **6** was assessed (Figure 4A).

Focusing on 36 nM and 1 μM **6**, concentrations equal to the reported IC_{50} and the amount used to assess cell-associated enzyme activity, it was shown that concentrations of PREP equal to 0.01- to 100-fold the concentration of FAP had no significant effect on the observed inhibition by **6**. In the case of PREP specific inhibition by **22**, similar results would be

NIH-PA Author Manuscript

NIH-PA Author Manuscript

NIH-PA Author Manuscript

anticipated given that **22** is much more selective for PREP over FAP than **6** is for FAP over PREP.

In order to determine if this range covers the enzyme activities associated with the cells used for the experiment in Figure 3, their FAP and PREP activities were measured and the relative concentrations of each calculated using a standard curve prepared from purified enzyme (Figure 4B). This yielded an FAP to PREP ratio of 1:1.5, well within the range tested in Figure 4A, further validating the cell-based results.

Cytotoxicity of 6 in mFAP Transfected Cells

Previously, it was discussed that inhibition of FAP activity in vivo has been associated with antitumor activity in a number of mouse tumor models.[16,17,20] Consequently, the cytotoxicity of **6** in mFAP transfected HEK293 cells was assessed, as these cells are known to express FAP and to represent a cell line that has been shown to rely on FAP activity for maximal tumor growth in vivo[17] (Figure 5). No cytotoxicity was observed in this assay. This does not necessarily prove that inhibition of FAP by **6** would not have an effect in vivo, however, as **20** has been shown to lack cytotoxicity against several tumor cell lines while still attenuating tumor growth in vivo in mice inoculated with those same cells.[20] In partial agreement with this, 20 was also shown here to lack cytotoxicity. Conversely, bortezomib, which represents a class of boronic acid inhibitors that target the proteasome, has been shown to be cytotoxic to cells in vitro and in vivo and was thus used here as a positive control.[39] These results suggest that any reduction in tumor volume resulting from FAP inhibition in vivo must be mediated by more complex pathways than those that can be mimicked using a cell-based assay alone.

CONCLUSIONS

Here we report the first FAP inhibitor, **6**, that combines low nanomolar potency with selectivity against both the DPPs and PREP, as well as **22**, a corresponding potent and specific inhibitor for PREP. Both are boronic acid based inhibitors, demonstrating that high selectivity can be achieved with the use of this electrophile, notwithstanding beliefs to the contrary. These inhibitors should prove to be useful in helping to elucidate the biological function of these important enzymes and to evaluate their potential as drug targets.

EXPERIMENTAL SECTION

Inhibitor Synthesis

Compound identities were confirmed via ^{1}H NMR and LC/MS, using the HPLC aspect of the latter to assess a level of relative purity of ≥95% for each inhibitor. Specifically, NMR spectra of the compounds in D_2O were recorded on a Bruker Avance 300 MHz spectrometer with a 5 mm dual 1H/X probe. Chemical shifts were reported relative to DSS. Mass spectra and HPLC retention times were recorded on a Hewlett-Packard HP LC/MSD system with UV detector (monitoring at 215 and 254 nm), using a Discovery C18 569232-U RP-HPLC column (12.5 cm, 4.6 mm, 5 μm) with solvent gradient A (water, 0.1% TFA) and B (acetonitrile, 0.08% TFA) flowing at 0.5 mL/min. Unless otherwise noted, all HPLC

NIH-PA Author Manuscript

NIH-PA Author Manuscript

NIH-PA Author Manuscript

retention times are given for an eluent gradient of 2% B for the first 5 min, 2–98% B over 10 min, and 98% B for the final 5 min.

Dipeptide Boronic Acid Synthesis

Synthesis of the X-boroPro dipeptides (**1** and **20**) was performed essentially as described previously[40] except that the initial coupling step was performed with HATU/DIPEA rather than EDC/HOBt, and the N- and C-terminal protection groups of the *N*-Boc-(*S*)-X-(*R*)-boroPro-(1*S*,2*S*,3*R*,5*S*)-pinanediol ester products were removed simultaneously. For the latter, to a stirred solution of the protected product in CH_2Cl_2 cooled to −78 °C, an equimolar amount of a 1.0 M solution of BCl_3 in CH_2Cl_2 was added. After 1 h, the product was extracted into water and purified on a Supelco Discovery-C18 column, eluting with water (0.1% TFA) and acetonitrile (0.08% TFA). Lyophilization yielded the free dipeptide boronic acids.

Glycinyl-(*R*)-boroproline (1)

^{1}H NMR (D_2O) δ 1.69–2.07 (m, 4H, BCHCH_2CH_2), 3.03–3.05 (m, 1H, CH_2C*H*B), 3.36–3.50 (m, 2H, CH_2CH_2N), 3.88 (s, 2H, H_2NCH_2CO). ^{13}C NMR (D_2O) δ 29.13, 29.53, 42.89, 49.11, 50.12, 166.89. ^{11}B NMR (D_2O) δ 11.03. LC–MS (ESI$^+$) *m/z* (rel intensity): 309.2, [2 × (M − H_2O) + H^+]; 155.2, [M − H_2O + H^+]. t_R = 5.2 min.

(*S*)-Valinyl-(*R*)-boroproline (20)

^{1}H NMR (D_2O) δ 0.98 (d, *J* = 6.9 Hz, 3H, CH_3CHCH_3), 1.08 (d, *J* = 6.9 Hz, 3H, CH_3CHCH_3), 1.60–2.34 (m, 5H, CH_3C*H*CH_3 and BCHCH_2CH_2), 3.03–3.09 (m, 1H, CH_2C*H*B), 3.43–3.75 (m, 2H, CH_2CH_2N), 4.12 (d, *J* = 6.3 Hz, 1H, H_2NC*H*CO). LC–MS (ESI$^+$) *m/z* (rel intensity): 393.3, [2 × (M − H_2O) + H^+]; 197.1, [M − H_2O + H^+], t_R = 11.1 min.

N-Terminally Blocked Dipeptide Boronic Acids

Synthesis of the N-terminally blocked X-boroPro dipeptides was similar to that of the dipeptide boronic acids but fell under two synthetic schemes, specifically, those that coupled the N-terminal blocking group to the P_2 residue first (**2**, **16**, and **19**) and those that coupled the P_1 and P_2 residues in the initial step, followed by the addition of the N-terminal blocking group (**5**–**15**, **17**, **18**, and **22**). The coupling methods for the blocking group additions, as well as descriptions of the specific chemical building blocks, are highlighted in Table 6. In the cases of **3**, **4**, and **21**, the P_2 residues with the desired N-terminal blocking group were commercially available, and these were coupled directly to the pinanediol protected P_1 boroproline residue.

N-(1-Naphthalenecarbonyl)glycinyl-(*R*)-boroproline (2)

^{1}H NMR (D_2O) δ 1.73–2.13 (m, 4H, BCHCH_2CH_2), 3.08–3.14 (m, 1H, CH_2C*H*B), 3.55–3.74 (m, 2H, CH_2CH_2N), 4.25–4.39 (d, *J* = 15.2 Hz, 2H, HNCH_2CO), 7.59–7.76 (m, 4H, aromatic H), 8.00–8.18 (m, 3H, aromatic H). LC–MS (ESI$^+$) *m/z* (rel intensity): 617.3, [2 × (M − H_2O) + H^+]; 309.2, [M − H_2O + H^+], t_R = 14.4 min.

NIH-PA Author Manuscript

NIH-PA Author Manuscript

NIH-PA Author Manuscript

N-Acetyl-(*R*)-alaninyl-(*R*)-boroproline (3)

^{1}H NMR (D_2O) δ 1.30–1.32 (d, J = 7.0 Hz, 3H, HNCHCH_3), 1.56–2.09 (m, 4H, BCHCH_2CH_2), 2.96–2.97 (m, 1H, CH_2C*H*B), 3.58–3.63 (m, 2H, CH_2CH_2N), 4.25–4.39 (q, J = 7.0 Hz, 3H, H_3CO). LC–MS (ESI$^+$) *m/z* (rel intensity): 421.2, [2 × (M − H_2O) + H^+]; 251.3, [M + Na^+]; 211.3, [M − H_2O + H^+], t_R = 12.2 min.

1-(2-(1-Oxoisoindolin-2-acetyl)-(*R*)-boroproline (4)

^{1}H NMR (D_2O) δ 1.67–2.07 (m, 4H, BCHC$H_2$$CH_2$), 2.99–3.04 (m, 1H, CH_2C*H*B), 3.47–3.62 (m, 2H, CH_2CH_2N), 4.41 (s, 2H, CCH_2N), 4.51 (s, 2H, HNCH_2CO), 7.49–7.76 (m, 4H, aromatic H). LC–MS (ESI$^+$) *m/z* (rel intensity): 541.4, [2 × (M − H_2O) + H^+]; 271.1, [M − H_2O + H^+], t_R = 8.4 min.

N-(Pyridine-4-carbonyl)glycinyl-(*R*)-boroproline (5)

^{1}H NMR (D_2O) δ 1.52–2.13 (m, 4H, BCHCH_2CH_2), 2.91–3.02 (m, 1H, CH_2C*H*B), 3.36–3.64 (m, 2H, CH_2CH_2N), 4.23 (s, 2H, HNCH_2CO), 8.33–8.35 (d, J = 5.4 Hz, 2H, aromatic H), 8.91–8.93 (d, J = 5.4 Hz, 2H, aromatic H). LC–MS (ESI$^+$) *m/z* (rel intensity): 519.2, [2 × (M − H_2O) + H^+]; 260.1, [M − H_2O + H^+], t_R = 11.9 min.

N-(Pyridine-4-carbonyl)-(*R*)-alaninyl-(*R*)-boroproline (6)

^{1}H NMR (D_2O) δ 1.45–1.47 (d, 3H, HNCHCH_3), 1.68–2.16 (m, 4H, BCHCH_2CH_2), 2.98–3.04 (m, 1H, CH_2C*H*B), 3.66–3.71 (m, 2H, CH_2CH_2N), 4.83–4.86 (m, 1H, HNC*H*CO), 8.36–8.38 (d, 2H, aromatic H), 8.94–8.96 (d, 2H, aromatic H). LC–MS (ESI$^+$) *m/z* (rel intensity): 547.2, [2 × (M − H_2O) + H^+]; 274.1, [M − H_2O + H^+], t_R = 12.0 min.

N-(Benzoyl)-(*R*)-alaninyl-(*R*)-boroproline (7)

^{1}H NMR (D_2O) δ 1.38–1.51 (d, 3H, HNCHCH_3), 1.60–2.24 (m, 4H, BCHCH_2CH_2), 2.93–3.08 (m, 1H, CH_2C*H*B), 3.62–3.77 (m, 2H, CH_2CH_2N), 4.70–4.85 (m, 1H, HNC*H*CO), 7.49–7.82 (m, 5H, aromatic H). LC–MS (ESI$^+$) *m/z* (rel intensity): 545.3, [2 × (M − H_2O) + H^+]; 273.1, [M − H_2O + H^+], t_R = 13.9 min.

N-(Pyridine-3-carbonyl)-(*R*)-alaninyl-(*R*)-boroproline (8)

^{1}H NMR (D_2O) δ 1.38–1.51 (d, 3H, HNCHCH_3), 1.58–2.20 (m, 4H, BCHCH_2CH_2), 2.79–3.05 (m, 1H, CH_2C*H*B), 3.59–3.74 (m, 2H, CH_2CH_2N), 4.72–4.87 (m, 1H, HNC*H*CO), 8.12–8.23 (m, 1H, aromatic H), 8.94–9.03 (m, 2H, aromatic H), 9.18–9.21 (s, 1H, aromatic H). The HPLC retention time is for an eluent gradient of 2% B for the first 3 min, 2–98% B over 6 min, and 98% B for the final 4 min. LC–MS (ESI$^+$) *m/z* (rel intensity): 547.2, [2 × (M − H_2O) + H^+]; 274.1, [M − H_2O + H^+], t_R = 7.3 min.

N-(Pyridine-3-fluoro-4-carbonyl)-(*R*)-alaninyl-(*R*)-boroproline (9)

^{1}H NMR (D_2O) δ 1.41–1.50 (d, 3H, HNCHCH_3), 1.61–2.22 (m, 4H, BCHCH_2CH_2), 2.89–3.04 (m, 1H, CH_2C*H*B), 3.59–3.74 (m, 2H, CH_2CH_2N), 4.79–4.84 (m, 1H, HNC*H*CO), 8.02–8.09 (m, 1H, aromatic H), 8.69–8.74 (d, 1H, aromatic H), 8.80–8.84 (d, 1H, aromatic H). The HPLC retention time is for an eluent gradient of 2% B for the first 3 min, 2–98% B

NIH-PA Author Manuscript

NIH-PA Author Manuscript

NIH-PA Author Manuscript

over 3 min, and 98% B for the final 5 min. LC–MS (ESI$^+$) *m/z* (rel intensity): 583.2, [2 × (M − H_2O) + H^+]; 292.0, [M − H_2O + H^+], t_R = 7.2 min.

N-(Pyridine-3-chloro-4-carbonyl)-(*R*)-alaninyl-(*R*)-boroproline (10)

^{1}H NMR (D_2O) δ 1.34–1.46 (d, 3H, HNCHCH_3), 1.62–2.21 (m, 4H, BCHCH_2CH_2), 2.91–3.04 (m, 1H, CH_2C*H*B), 3.62–3.74 (m, 2H, CH_2CH_2N), 4.77–4.82 (m, 1H, HNC*H*CO), 7.89–7.93 (d, 1H, aromatic H), 8.71–8.76 (d, 1H, aromatic H), 8.81–8.85 (s, 1H, aromatic H). The HPLC retention time is for an eluent gradient of 2% B for the first 3 min, 2–98% B over 3 min, and 98% B for the final 5 min. LC–MS (ESI$^+$) *m/z* (rel intensity): 615.2, [2 × (M − H_2O) + H^+]; 308.0, [M − H_2O + H^+], t_R = 7.6 min.

N-(Pyridine-2-fluoro-4-carbonyl)-(*R*)-alaninyl-(*R*)-boroproline (11)

^{1}H NMR (D_2O) δ 1.37–1.49 (d, 3H, HNCHCH_3), 1.61–2.21 (m, 4H, BCHCH_2CH_2), 2.93–3.03 (m, 1H, CH_2C*H*B), 3.62–3.69 (m, 2H, CH_2CH_2N), 4.61–4.80 (m, 1H, HNC*H*CO), 7.31–7.82 (m, 2H, aromatic H), 8.26–8.33 (d, 1H, aromatic H), 8.81–8.85 (s, 1H, aromatic H). The HPLC retention time is for an eluent gradient of 2% B for the first 3 min, 2–98% B over 3 min, and 98% B for the final 5 min. LC–MS (ESI$^+$) *m/z* (rel intensity): 583.3, [2 × (M − H_2O) + H^+]; 292.2, [M − H_2O + H^+], t_R = 7.1 min.

N-(Pyridine-2-chloro-4-carbonyl)-(*R*)-alaninyl-(*R*)-boroproline (12)

^{1}H NMR (D_2O) δ 1.36–1.47 (d, 3H, HNCHCH_3), 1.59–2.11 (m, 4H, BCHCH_2CH_2), 2.88–3.01 (m, 1H, CH_2C*H*B), 3.62–3.71 (m, 2H, CH_2CH_2N), 4.66–4.79 (m, 1H, HNC*H*CO), 7.66–7.71 (d, 1H, aromatic H), 7.76–7.80 (s, 1H, aromatic H), 8.44–8.49 (d, 1H, aromatic H). The HPLC retention time is for an eluent gradient of 2% B for the first 3 min, 2–98% B over 3 min, and 98% B for the final 5 min. LC–MS (ESI$^+$) *m/z* (rel intensity): 615.1, [2 × (M − H_2O) + H^+]; 308.0, [M − H_2O + H^+], t_R = 7.7 min.

N-(Quinoline-4-carbonyl)-(*R*)-alaninyl-(*R*)-boroproline (13)

^{1}H NMR (D_2O) δ 1.45–1.48 (d, J = 6.9 Hz, 3H, HNCHCH_3), 1.70 – 2.13 (m, 4H, BCHCH_2CH_2), 3.02–3.07 (m, 1H, CH_2C*H*B), 3.72–3.77 (m, 2H, CH_2CH_2N), 4.88–4.97 (m, 1H, HNC*H*CO), 7.97–8.33 (m, 5H, aromatic H), 9.18–9.20 (d, 1H, NC*H*CH, aromatic H). LC–MS (ESI$^+$) *m/z* (rel intensity): 647.3, [2 × (M − H_2O) + H^+]; 324.3, [M − H_2O + H^+], t_R = 12.8 min.

N-(Quinoline-4-carbonyl)-(*R*)-serinyl-(*R*)-boroproline (14)

^{1}H NMR (D_2O) δ 1.75–2.20 (m, 4H, BCHCH_2CH_2), 3.05–3.11 (m, 1H, CH_2C*H*B), 3.78–3.82 (m, 2H, CH_2CH_2N), 3.87–4.03 (m, 2H, CHCH_2OH), 5.13–5.17 (m, 1H, HNC*H*CO), 8.01–8.36 (m, 5H, aromatic H), 9.21–9.23 (d, 1H, NC*H*CH, aromatic H). LC–MS (ESI$^+$) *m/z* (rel intensity): 679.3, [2 × (M − H_2O) + H^+]; 340.2, [M − H_2O + H^+], t_R = 12.4 min.

N-(Quinoline-4-carbonyl)-(*R*)-methioninyl-(*R*)-boroproline (15)

^{1}H NMR (D_2O) δ 1.74–2.22 (m, 4H, BCHCH_2CH_2), 2.04–2.22 (m, 5H, CHC$H_2$$CH_2SCH_3$), 2.67–2.75 (m, 1H, CH_2C*H*B), 2.67–3.10 (m, 2H, CH_2CH_2N), 3.79–3.83 (m, 2H, $CH_2$$CH_2$S), 5.14–5.19 (m, 1H, HNC*H*CO), 8.01–8.32 (m, 5H, aromatic H), 9.21–9.23 (d,

NIH-PA Author Manuscript

NIH-PA Author Manuscript

NIH-PA Author Manuscript

1H, NC*H*CH, aromatic H). LC–MS (ESI$^+$) *m/z* (rel intensity): 767.3, [2 × (M − H_2O) + H^+]; 384.5, [M − H_2O + H^+], t_R = 12.9 min.

N-(Quinoline-4-carbonyl)-(*R*)-ethyl(glycinyl)-(*R*)-boroproline (16)

^{1}H NMR (D_2O) δ 1.02–1.07 (m, 3H, $CHCH_2CH_3$), 1.72–1.91 (m, 2H, $CHCH_2CH_3$), 1.72–2.16 (m, 4H, BCHCH_2CH_2), 3.03–3.08 (m, 1H, CH_2C*H*B), 3.76–3.81 (m, 2H, CH_2CH_2N), 4.84–4.89 (m, 1H, HNC*H*CO), 7.99–8.32 (m, 5H, aromatic H), 9.20–9.21 (d, 1H, NC*H*CH, aromatic H). LC–MS (ESI$^+$) *m/z* (rel intensity): 675.3, [2 × (M − H_2O) + H^+]; 338.4, [M − H_2O + H^+], t_R = 13.2 min.

N-(Quinoline-4-carbonyl)-(*R*)-propyl(glycinyl)-(*R*)-boroproline (17)

^{1}H NMR (D_2O) δ 0.93–0.98 (m, 3H, CH_2CH_2CH3), 1.45–1.52 (m, 2H, $CH_2CH_2CH_3$), 1.73–1.84 (m, 2H, $CHCH_2CH_2$), 1.73–2.14 (m, 4H, BCHCH_2CH_2), 3.01–3.07 (m, 1H, CH_2C*H*B), 3.75–3.80 (m, 2H, CH_2CH_2N), 4.91–4.96 (m, 1H, HNC*H*CO), 7.99–8.30 (m, 5H, aromatic H), 9.20–9.21 (d, 1H, NC*H*CH, aromatic H). LC–MS (ESI$^+$) *m/z* (rel intensity): 703.5, [2 × (M − H_2O) + H^+]; 352.3, [M − H_2O + H^+], t_R = 13.7 min.

N-(Quinoline-4-carbonyl)-(*R*)-butyl(glycinyl)-(*R*)-boroproline (18)

^{1}H NMR (D_2O) δ 0.86–0.91 (m, 3H, CH_2CH_2CH3), 1.34–1.45 (m, 4H, $CH_2CH_2CH_2CH_3$), 1.81–1.85, (m, 2H, $CHCH_2CH_2$), 1.81–2.14 (m, 4H, BCHCH_2CH_2), 3.01–3.07 (m, 1H, CH_2C*H*B), 3.74–3.81 (m, 2H, CH_2CH_2N), 4.89–4.94 (m, 1H, HNC*H*CO), 7.99–8.30 (m, 5H, aromatic H), 9.19–9.21 (d, 1H, NC*H*CH, aromatic H). The HPLC retention time is for an eluent gradient 2% B for the first 3 min, 2–98% B over 6 min and 98%B for the final 4 min. LC–MS (ESI$^+$) *m/z* (rel intensity): 365.7, [M − H_2O + H^+], t_R = 8.5 min.

N-(Quinoline-4-carbonyl)-(*R*)-phenyl(glycinyl)-(*R*)-boroproline (19)

^{1}H NMR (D_2O) δ 1.70–1.72 (m, 2H, BCHCH_2CH_2), 1.73–2.00 (m, 2H, BCHCH_2CH_2), 2.99–3.06 (m, 1H, CH_2C*H*B), 3.26–3.68 (m, 2H, CH_2CH_2N), 6.00 (s, 1H, HNC*H*CO), 7.42–7.46 (m, 5H, phenyl H), 7.93–8.31 (m, 5H, aromatic H), 9.13–9.15 (d, 1H, NCHCH, aromatic H). LC–MS (ESI$^+$) *m/z* (rel intensity): 386.1, [M − H_2O + H^+], t_R = 14.1 min.

N-(Pyridine-3-carbonyl)glycinyl-(*R*)-boroproline (21)

^{1}H NMR (D_2O) δ 1.68–2.10 (m, 4H, BCHCH_2CH_2), 3.02–3.08 (m, 1H, CH_2C*H*B), 3.47–3.69 (m, 2H, CH_2CH_2N), 4.29 (s, 2H, HNCH_2CO), 8.18–8.22 (m, 1H, NCHC*H*CH, aromatic H), 8.94–8.96 (m, 2H, NC*H*CHC*H*, aromatic H), 9.22 (s, 1H, NC*H*CCO, aromatic H). LC–MS (ESI$^+$) *m/z* (rel intensity): 519.2, [2 × (M − H_2O) + H^+]; 260.1, [M − H_2O + H^+], t_R = 11.5 min.

N-(Pyridine-3-carbonyl)-(*R*)-valinyl-(*R*)-boroproline (22)

^{1}H NMR (D_2O) δ 0.96–1.03 (m, 6H, CHCH(CH_3)$_2$), 1.69–2.15 (m, 4H, BCHCH_2CH_2), 2.15–2.22 (m, 1H, CHCH(CH_3)$_2$), 2.95–2.99 (m, 1H, CH_2C*H*B), 3.57–4.01 (m, 2H, CH_2CH_2N), 4.61–4.63 (m, 1H, HNC*H*CO), 8.16–8.21 (m, 1H, NC*H*CHC*H*, aromatic H), 8.92–8.95 (m, 2H, NC*H*CHC*H*, aromatic H), 9.16 (s, 1H, NCHCCO, aromatic H). The HPLC retention time is for an eluent gradient 2% B for the first 3 min, 2–98% B over 6 min,

NIH-PA Author Manuscript

NIH-PA Author Manuscript

NIH-PA Author Manuscript

and 98% B for the final 4 min. LC–MS (ESI^+) *m/z* (rel intensity): 602.4, [2 × (M − H_2O)]; 302.2, [M − H_2O + H^+], t_R = 6.7 min.

Synthesis of Bortezomib

Bortezomib was synthesized as described previously.[41]

Biological Materials

The peptide libraries XPYSWS-NH_2, Ac-XPYSWS-NH_2, GXYSWS-NH_2, and Ac-GXYSWS-NH_2, where X represents all natural amino acids except cysteine were synthesized by the Tufts University Core Facility. The DPPIV enzyme used for the specificity studies was previously purified by our laboratory at Tufts University from human placenta, and the purified human FAP enzyme used for these studies was kindly provided by Syrxx, Inc. For the in vitro IC_{50} determination assays, recombinant human DPPIV, DPP9, FAP, and PREP were purchased from R&D Systems, and DPP8 was from Biomol International. Buffer systems used were A (25 mM Tris, pH 8.0), B (50 mM Tris, pH 7.5), C (50 mM Tris, 140 mM NaCl, pH 7.5), D (25 mM Tris, 250 mM NaCl, pH 7.5), and E (20 mM Tris, 20 mM KCl, pH 7.4). Fluorogenic substrates were Gly-Pro-AMC, Z-Gly-Pro-AMC, or Suc-Gly-Pro-AMC purchased from Bachem or an N-terminally blocked FAP specific substrate.[42] The cell culture medium was RPMI 1640 without phenol red and supplemented with 2 mM L-glutamine, 10 mM HEPES, 1 mM sodium pyruvate, 4500 mg/L glucose, 100 IU/mL penicillin, and 100 μg/mL streptomycin.

Substrate Specificity Assay

Peptide libraries (0.21 mM) were incubated for 24 h with 1 nM FAP in buffer E at 37 °C. The reaction was quenched by the addition of 1.2 N HCl. The samples were analyzed by reverse-phase HPLC–MS on a Thermo Finnigan LCQ Duo, quantifying the peaks in the resulting base peak chromatograms. Relative cleavage values were determined by comparing the postquench abundance of intact peptides to those in the initial library.

In Vitro Enzyme IC_{50} Assays

Enzymatic activity of DPPIV, DPP8, DPP9, FAP, and PREP was measured at 25 °C on a Molecular Devices M2^e multidetection microtiter plate reader, monitoring the fluorescence at an excitation wavelength of 380 nm and an emission wavelength of 460 nm. The substrate was either H-Gly-Pro-AMC for the DPPIV, DPP8, and DPP9 assays or Z-Gly-Pro-AMC for the FAP and PREP assays. The reaction mixture contained 25 μM substrate, enzyme, buffer A (DPPIV and DPP9), buffer B (DPP8), buffer C (FAP), or buffer D (PREP) and a suitable amount of inhibitor (ranging between 10^{-4} and 10^{-11} M) in a total volume of 210 μL. The final enzyme concentrations were 0.1, 0.8, 0.4, 1.2, and 0.6 nM for DPPIV, DPP8, DPP9, FAP, and PREP, respectively. The IC_{50} value is defined as the concentration of inhibitor required to reduce the enzyme activity by 50% after a 10 min preincubation with the enzyme at 25 °C prior to addition of the substrate.

Inhibitor stock solutions (100 mM) were prepared in either a pH 2.0 HCl solution for compounds **1** and **20** or DMSO. Those prepared in pH 2.0 solution were preincubated at 25 °C for 4 h prior to dilution. Immediately prior to the commencement of the experiment, the

NIH-PA Author Manuscript

NIH-PA Author Manuscript

NIH-PA Author Manuscript

100 mM stocks were further diluted to 10^{-3} M in the appropriate assay buffer, from which 1:10 serial dilutions were prepared. All inhibitors were tested in triplicate.

Molecular Modeling of 6 Bound to FAP

Using Insight II (version 2005.03) and beginning with the homologous X-ray crystallographic structure of the DPPIV tetrahedral intermediate complexed with diprotinA (PDB accession code 1NU8), the -boroPro moiety of **6** was positioned in the similarly shaped hydrophobic S_1 pocket of FAP (PDB accession code 1Z68). The boron was placed at nearly the same distance, 1.6 Å, from the Ser^{624} oxygen as previously reported B–O bonds. Tetrahedral angles for boron were maintained as closely as possible, utilizing the free rotation of ligand C_α–B and enzyme Ser^{624} C_α–C_β single bonds. The ligand **6** dihedral angles were varied sequentially from Ψ_2 to ϕ_2 of the D-alanyl group to Ψ_3 of the 4-pyridylcarbonyl group to optimize possible hydrogen bond receptors for the pyridinium N–H^+ group ($\Psi_3 = -160°$, $\omega_3 = -177°$, $\phi_2 = 94°$, $\Psi_2 = 65°$, $\omega_2 = -177°$, $\phi_1 = -73°$). This placed the pyridinium N–H^+ proton in position for hydrogen bonding to the backbone carbonyl oxygen atom of Glu^{204}, with an H–O distance of 1.87 Å and an N–H–O angle of 121°.

Characterization of Competitive/Noncompetitive Inhibition

The enzyme kinetics for FAP or PREP with or without varying concentrations ((0.5–2)IC_{50}) of **6** or **22** were measured in the appropriate assay buffer at 37 °C, using Suc-GP-AMC at concentrations equivalent to (0.1–5)× its respective K_m values for these enzymes. The enzyme concentration was 5 nM. **6** was added concurrent with the substrate and enzyme, while **22** was allowed to preincubate with the enzyme for 10 min prior to the addition of the substrate due to observed slow binding kinetics. The fluorescence was continuously monitored at excitation and emission wavelengths of 380 and 460 nm, respectively. Standard curves for 7-amino-4 methyl-coumarin (Aldrich) were used to convert the fluorescence units into the concentration of the released fluorophore. From this, the slope of [AMC] versus time yielded the reaction rate for each condition. The resulting Lineweaver–Burk plots were prepared by plotting $1/V$, where V was equal to the reaction rate calculated above, versus 1/[S] and were analyzed with a linear regression analysis, using GraphPad software. K_i values were also determined using GraphPad software, fitting the V vs [S] results to a competitive inhibition analysis.

Inhibition of Cellular Enzyme Activity in HEK293 Cells

Mock or murine FAP (mFAP) transfected HEK293 cells were kindly provided by Jonathan Cheng from the Fox Chase Cancer Center. The cells were equilibrated in RPMI 1640 at a density of 25 000 cells/well, treated with 1 μM **2**, **6**, **22**, or RPMI 1640 alone, and allowed to incubate for 15 min at 37 °C. The substrate was 25 μM Z-Gly-Pro-AMC. The fluorescence was measured at 37 °C, monitoring an excitation wavelength of 380 nm and an emission wavelength of 460 nm. The percent activity was determined versus the RPMI 1640 control.

In Vitro Mixed FAP and PREP Inhibition Assay

Enzymatic activity of 1 nM FAP combined with 0.01–100 nM PREP was measured at 25 °C, monitoring the fluorescence at an excitation wavelength of 380 nm and an emission

NIH-PA Author Manuscript

NIH-PA Author Manuscript

NIH-PA Author Manuscript

wavelength of 460 nm. The substrate was the N-terminally blocked FAP specific substrate, so as to be able to differentiate FAP activity in the presence of PREP. The final reaction mixture contained 25 μM substrate, enzyme, a 1:1 mixture of buffer C and buffer D, and either 36 nM or 1 μM **6** in a total volume of 210 μL. The enzymes were allowed to preincubate with the inhibitor for 10 min at room temperature prior to addition of the substrate. The percent of FAP activity was determined based on a simultaneously run control for each condition, which lacked treatment with the inhibitor.

Measurement of FAP and PREP Activity in HEK293 Cells

Both mock and mFAP transfected HEK293 cells were equilibrated in RPMI 1640 at a density of 25 000 cells/well. The mock transfected cells were treated with 25 μM Z-GP-AMC, and the mFAP transfected cells were treated with 50 μM N-terminally blocked FAP specific inhibitor in a total volume of 200 μL/well. The fluorescence was measured at 37 °C, monitoring an excitation wavelength of 380 nm and an emission wavelength of 460 nm. To calculate the relative cellular PREP and FAP concentrations, standard activity curves were prepared for each using varying concentrations of purified enzyme and Z-GP-AMC for PREP and the N-terminally blocked FAP specific substrate for FAP. The relative concentration of active enzyme associated with the cells was calculated via interpolation from the standard curves and the measured cellular activity.

Cell Viability Assay

mFAP transfected HEK293 cells were equilibrated in RPMI 1640 at a density of 25 000 cells/well. Cells were treated with RPMI 1640 alone or varying concentrations of **6**, **20**, or bortezomib (ranging between 10^{-3} and 10^{-11} M) in a final assay volume of 100 μL. Following a 48 h incubation at 37 °C, all wells were treated with CellTiter–Blue reagent from Promega and incubated an additional 2 h at 37 °C and the fluorescence was measured, monitoring an excitation wavelength of 560 nm and an emission wavelength of 590 nm. Percent cell viability relating to the inhibitors was determined versus the cells treated with RPMI 1640 alone.

Acknowledgments

This work was supported by Arisaph Pharmaceuticals, Inc.

ABBREVIATIONS USED

FAP	fibroblast activation protein
PREP	prolyl oligopeptidase
DPPIV	dipeptidyl peptidase IV
DPPII	dipeptidyl peptidase II
DPP8	dipeptidyl peptidase 8
DPP9	dipeptidyl peptidase 9
GLP-1	glucagon-like peptide 1

NIH-PA Author Manuscript

NIH-PA Author Manuscript

NIH-PA Author Manuscript

GIP	glucose-dependent insulinotropic peptide
K_i	inhibition constant
IC_{50}	median inhibition concentration

REFERENCES

(1). Garin-Chesa P, Old LJ, Rettig WJ. Cell surface glycoprotein of reactive stromal fibroblasts as a potential antibody target in human epithelial cancers. Proc. Natl. Acad. Sci. U.S.A. 1990; 87:7235–7239. [PubMed: 2402505]

(2). Rettig WJ, Garin-Chesa P, Healey JH, Su SL, Ozer HL, Schwab M, Albino AP, Old LJ. Regulation and heteromeric structure of the fibroblast activation protein in normal and transformed cells of mesenchymal and neuroectodermal origin. Cancer Res. 1993; 53:3327–3335. [PubMed: 8391923]

(3). Rettig WJ, Su SL, Fortunato SR, Scanlan MJ, Raj BK, Garin-Chesa P, Healey JH, Old LJ. Fibroblast activation protein: purification, epitope mapping and induction by growth factors. Int. J. Cancer. 1994; 58:385–392. [PubMed: 7519584]

(4). Park JE, Lenter MC, Zimmermann RN, Garin-Chesa P, Old LJ, Rettig WJ. Fibroblast activation protein, a dual specificity serine protease expressed in reactive human tumor stromal fibroblasts. J. Biol. Chem. 1999; 274:36505–36512. [PubMed: 10593948]

(5). Connolly BA, Sanford DG, Chiluwal AK, Healey SE, Peters DE, Dimare MT, Wu W, Liu Y, Maw H, Zhou Y, Li Y, Jin Z, Sudmeier JL, Lai JH, Bachovchin WW. Dipeptide boronic acid inhibitors of dipeptidyl peptidase IV: determinants of potency and in vivo efficacy and safety. J. Med. Chem. 2008; 51:6005–6013. [PubMed: 18783201]

(6). Maes M, Lambeir A, Gilany K, Senten K, Van der Veken P, Leiting B, Augustyns K, Scharpé S, De Meester I. Kinetic investigation of human dipeptidyl peptidase II (DPPII)-mediated hydrolysis of dipeptide derivitives and its identification as quiescent cell proline dipeptidase (QPP)/dipeptidyl peptidase 7 (DPP7). Biochem. J. 2005; 386:315–324. [PubMed: 15487984]

(7). Yoshimoto T, Fischl M, Orlowski RC, Walter R. Post-proline cleaving enzyme and post-proline dipeptidyl aminopeptidase. Comparison of two peptidases with high specificity for proline residues. J. Biol. Chem. 1978; 253:3708–3716. [PubMed: 649599]

(8). Levy MT, McCaughan GW, Abbott CA, Park JE, Cunningham AM, Muller E, Rettig WJ, Gorrell MD. Fibroblast activation protein: a cell surface dipeptidyl peptidase and gelatinase expressed by stellate cells at the tissue remodeling interface in human cirrhosis. Hepatology. 1999; 29:1768–1778. [PubMed: 10347120]

(9). Vanhoof G, Goossens F, De Meester I, Hendriks D, Scharpé S. Proline motifs in peptides and their biological processing. FASEB J. 1995; 9:736–744. [PubMed: 7601338]

(10). Mentlein R, Gallwitz B, Schmidt WE. Dipeptidyl-peptidase IV hydrolyses gastric inhibitory polypeptide, glucagon-like peptide-1(7-36)amide, peptide histidine methionine and is responsible for their degradation in human serum. Eur. J. Biochem. 1993; 214:829–835. [PubMed: 8100523]

(11). Kieffer TJ, McIntosh CH, Pederson RA. Degradation of glucose-dependent insulinotropic polypeptide and truncated glucagon-like peptide 1 in vitro and in vivo by dipeptidyl peptidase IV. Endocrinology. 1995; 136:3585–3596. [PubMed: 7628397]

(12). Choy M, Lam S. Sitagliptin: a novel drug for the treatment of type 2 diabetes. Cardiol. Rev. 2007; 15:264–271. [PubMed: 17700385]

(13). Cheng JD, Dunbrack RL Jr. Valianou M, Rogatko A, Alpaugh RK, Weiner LM. Promotion of tumor growth by murine fibroblast activation protein, a serine protease, in an animal model. Cancer Res. 2002; 62:4767–4772. [PubMed: 12183436]

(14). Scott AM, Wiseman G, Welt S, Adjei A, Lee FT, Hopkins W, Divgi CR, Hanson LH, Mitchell P, Gansen DN, Larson SM, Ingle JN, Hoffman EW, Tanswell P, Ritter G, Cohen LS, Bette P, Arvay L, Amelsberg A, Vlock D, Rettig WJ, Old LJ. A phase I dose-escalation study of

NIH-PA Author Manuscript

NIH-PA Author Manuscript

NIH-PA Author Manuscript

sibrotuzumab in patients with advanced or metastatic fibroblast activation protein-positive cancer. Clin. Cancer Res. 2003; 9:1639–1647. [PubMed: 12738716]

(15). Puré E. The road to integrative cancer therapies: emergence of a tumor-associated fibroblast protease as a potential therapeutic target in cancer. Expert Opin. Ther. Targets. 2009; 13:967–973. [PubMed: 19606930]

(16). Santos AM, Jung J, Aziz N, Kissil JL, Puré E. Targeting fibroblast activation protein inhibits tumor stromagenesis and growth in mice. J. Clin. Invest. 2009; 119:3613–3625. [PubMed: 19920354]

(17). Cheng JD, Valianou M, Canutescu AA, Jaffe EK, Lee HO, Wang H, Lai JH, Bachovchin WW, Weiner LM. Abrogation of fibroblast activation protein enzymatic activity attenuates tumor growth. Mol. Cancer Ther. 2005; 4:351–360. [PubMed: 15767544]

(18). Kraman M, Bambrough PJ, Arnold JN, Roberts EW, Magiera L, Jones JO, Gopinathan A, Tuveson DA, Fearon DT. Suppression of antitumor immunity by stromal cells expressing fibroblast activation protein-alpha. Science. 2010; 330:827–830. [PubMed: 21051638]

(19). Huang Y, Simms AE, Mazur A, Wang S, León NR, Jones B, Aziz N, Kelly T. Fibroblast activation protein-α promotes tumor growth and invasion of breast cancer cells through non-enzymatic functions. Clin. Exp. Metastasis. 2011; 28:567–579. [PubMed: 21604185]

(20). Adams S, Miller GT, Jesson MI, Watanabe T, Jones B, Wallner BP. PT-100, a small molecule dipeptidyl peptidase inhibitor, has potent antitumor effects and augments antibody-mediated cytotoxicity via a novel immune mechanism. Cancer Res. 2004; 64:5471–5480. [PubMed: 15289357]

(21). Edosada CY, Quan C, Wiesmann C, Tran T, Sutherlin D, Reynolds M, Elliott JM, Raab H, Fairbrother W, Wolf BB. Selective inhibition of fibroblast activation protein based on dipeptide substrate specificity. J. Biol. Chem. 2006; 281:7437–7444. [PubMed: 16410248]

(22). Tran T, Quan C, Edosada CY, Mayeda M, Wiesmann C, Sutherlin D, Wolf BB. Synthesis and structure–activity relationship of N-acyl-Gly-, N-acyl-Sar- and N-blocked-boroPro inhibitors of FAP, DPP4 and POP. Bioorg. Med. Chem. Lett. 2007; 17:1438–1442. [PubMed: 17174090]

(23). Tsai T, Yeh T, Chen X, Hsu T, Jao Y, Huang C, Song J, Huang Y, Chien C, Chiu J, Yen S, Tang H, Chao Y, Jiaang W. Substituted 4-caboxymethylpyroglutamic acid diamides as potent and selective inhibitors of fibroblast activation protein. J. Med. Chem. 2010; 53:6572–6583. [PubMed: 20718420]

(24). Ryabtsova O, Jansen K, Van Goethem S, Joossens J, Cheng JD, Lambeir A, De Meester I, Augustyns K, Van der Veken P. Acylated Gly-(2-cyano)pyrrolidines as inhibitors of fibroblast activation protein (FAP) and the issues of FAP/prolyl oligopeptidase (PREP)-selectivity. Bioorg. Med. Chem. Lett. 2012; 22:3412–3417. [PubMed: 22525314]

(25). Lee KN, Jackson KW, Christiansen VJ, Lee CS, Chun JG, McKee PA. Antiplasmin-cleaving enzyme is a soluble form of fibroblast activation protein. Blood. 2006; 107:1397–1404. [PubMed: 16223769]

(26). Tenorio-Laranga J, Venäläinen JI, Männistö PT, García-Horsman JA. Characterization of membrane-bound prolyl endopeptidase from brain. FEBS J. 2008; 275:4415–4427. [PubMed: 18657187]

(27). Irazusta J, Larrinaga G, González-Maeso J, Gil J, Meana JJ, Casis L. Distribution of prolyl endopeptidase activities in rat and human brain. Neurochem. Int. 2002; 40:337–345. [PubMed: 11792464]

(28). Myöhänen TT, Pyykkö E, Männistö PT, Carpen O. Distribution of prolyl oligopeptidase in human peripheral tissues and in ovarian and colorectal tumors. J. Histochem. Cytochem. 2012; 60:706–715. [PubMed: 22740343]

(29). Turk B. Targeting proteases: successes, failures and future prospects. Nat. Rev. Drug Discovery. 2006; 5:785–799.

(30). Singh J, Petter RC, Baillie TA, Whitty A. The resurgence of covalent drugs. Drug Discovery. 2011; 10:307–317. [PubMed: 21455239]

(31). Johnson DS, Weerapana E, Cravatt BF. Strategies for discovering and derisking covalent, irreversible enzyme inhibitors. Future Med. Chem. 2010; 2:949–964. [PubMed: 20640225]

NIH-PA Author Manuscript

NIH-PA Author Manuscript

NIH-PA Author Manuscript

(32). Sanderson PE. Small, noncovalent serine protease inhibitors. Med. Res. Rev. 1999; 19:179–197. [PubMed: 10189177]

(33). Bachovchin DA, Cravatt BF. The pharmacological landscape and therapeutic potential of serine hydrolases. Nat. Rev. Drug Discovery. 2012; 11:52–68.

(34). Edosada CY, Quan C, Tran T, Pham V, Wiesmann C, Fairbrother W, Wolf BB. Peptide substrate profiling defines fibroblast activation protein as an endopeptidase of strict Gly(2)-Pro(1)-cleaving specificity. FEBS Lett. 2006; 580:1581–1586. [PubMed: 16480718]

(35). Aggarwal S, Brennen WN, Kole TP, Schneider E, Topaloglu O, Yates M, Cotter RJ, Denmeade SR. Fibroblast activation protein peptide substrates identified from human collagen I derived gelatin cleavage sites. Biochemistry. 2008; 47:1076–1086. [PubMed: 18095711]

(36). Wolf BB, Quan C, Tran T, Wiesmann C, Sutherlin D. On the edge of validation—cancer protease fibroblast activation protein. Mini-Rev. Med. Chem. 2008; 8:719–727. [PubMed: 18537727]

(37). Fülöp V, Böcskei Z, Polgár L. Prolyl oligopeptidase; an unusual beta-propeller domain regulates proteolysis. Cell. 1998; 94:161–170. [PubMed: 9695945]

(38). Wang XM, Yu DMT, McCaughan W, Gorrell MD. Fibroblast activation protein increases apoptosis, cell adhesion, and migration by the LX-2 human stellate cell line. Hepatology. 2005; 42:935–945. [PubMed: 16175601]

(39). Sunwoo JB, Chen Z, Dong G, Yeh N, Bancroft CC, Sausville E, Adams J, Elliot P, Van Waes C. Novel proteasome inhibitor PS-341 inhibits activation of nuclear factor-κB cell survival, tumor growth, and angiogenesis in squamous cell carcinoma. Clin. Cancer Res. 2001; 7:1419–1428. [PubMed: 11350913]

(40). Coutts SJ, Kelly TA, Snow RJ, Kennedy CA, Barton RW, Adams J, Krolikowski DA, Freeman DM, Campbell SJ, Ksiazek JF, Bachovchin WW. Structure-activity relationships of boronic acid inhibitors of dipeptidyl peptidase IV. Variation of the P2 position of Xaa-boroPro dipeptides. J. Med. Chem. 1996; 39:2087–2094. [PubMed: 8642568]

(41). Milo LJ, Lai JH, Wu W, Liu Y, Maw H, Li Y, Jin Z, Shu Y, Poplawski SE, Wu Y, Sanford DG, Sudmeier JL, Bachovchin WW. Chemical and biological evaluation of dipeptidyl boronic acid proteasome inhibitors for use in prodrugs and pro-soft drugs targeting solid tumors. J. Med. Chem. 2011; 54:4365–4377. [PubMed: 21634429]

(42). Poplawski SE, Li Y, Shu Y, Zhang M, DiMare MT, Sanford DG, Lai JH, Cheng JD, Gorrell MD, Bachovchin WW. Unpublished data.

NIH-PA Author Manuscript

NIH-PA Author Manuscript

NIH-PA Author Manuscript

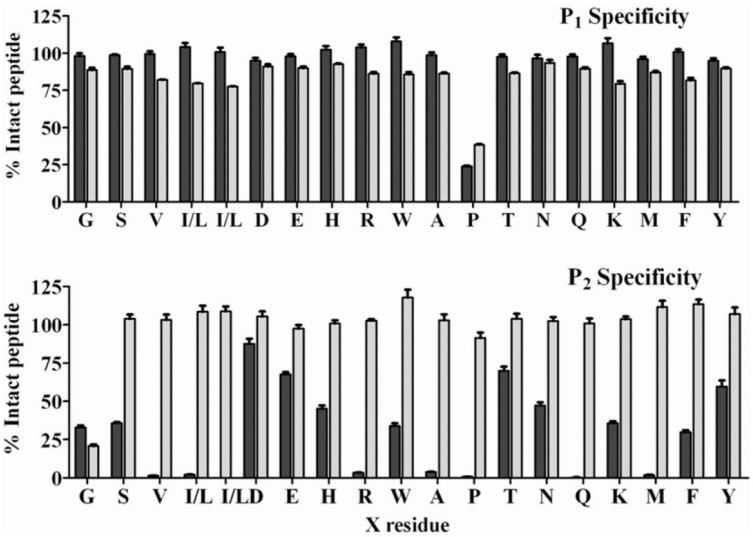

Figure 1.

P_1 and P_2 specificity of FAP. Percentage of intact peptide remaining following a 24 h incubation at 37 °C of FAP with either the GXYSWS-NH_2 or Ac-GXYSWS-NH_2 peptide library for P_1 analysis or the XPYSWS-NH_2 or Ac-XPYSWS-NH_2 peptide library for P_2 analysis. The dark columns represent the peptide libraries with a free N-terminus, while the light columns represent the acetyl blocked libraries. Error bars show the mean ± SEM.

NIH-PA Author Manuscript

NIH-PA Author Manuscript

NIH-PA Author Manuscript

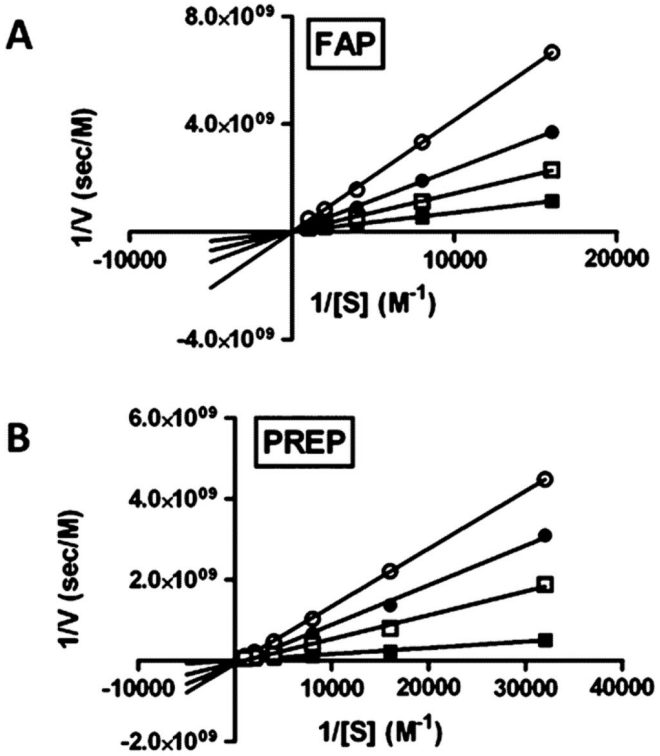

Figure 2.

Lineweaver–Burk plots for inhibition of FAP and PREP by 6. FAP (A) and PREP (B) either alone (closed squares) or with inhibitor concentrations equal to 0.5 IC_{50} (open squares), IC_{50} (closed squares), or 2 IC_{50} (open squares) were incubated with varying concentrations of Suc-GP-AMC ((0.1–5)K_m) at 37 °C.

NIH-PA Author Manuscript

NIH-PA Author Manuscript

NIH-PA Author Manuscript

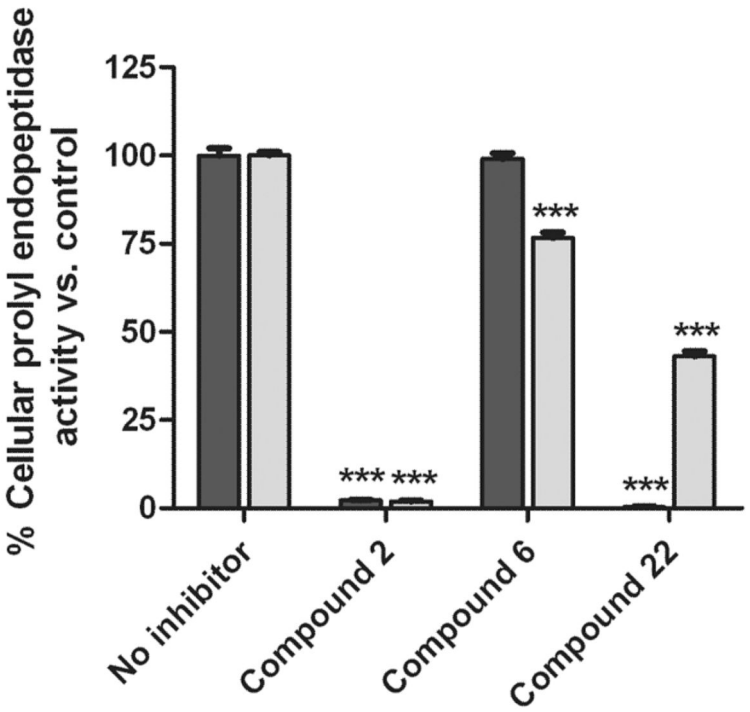

Figure 3.

Inhibition of cellular prolyl endopeptidase activity in mock and murine FAP transfected HEK293 cells. Mock (dark columns) and mFAP transfected (light columns) HEK293 cells were incubated with cell culture medium alone or 1 μM **2**, **6**, or **22** for 15 min at 37 °C. The endopeptidase activity was assessed via cleavage of a Z-GP-AMC substrate: ***, $P <$ 0.0001 vs no inhibitor control. Error bars show the mean ± SEM.

NIH-PA Author Manuscript

NIH-PA Author Manuscript

NIH-PA Author Manuscript

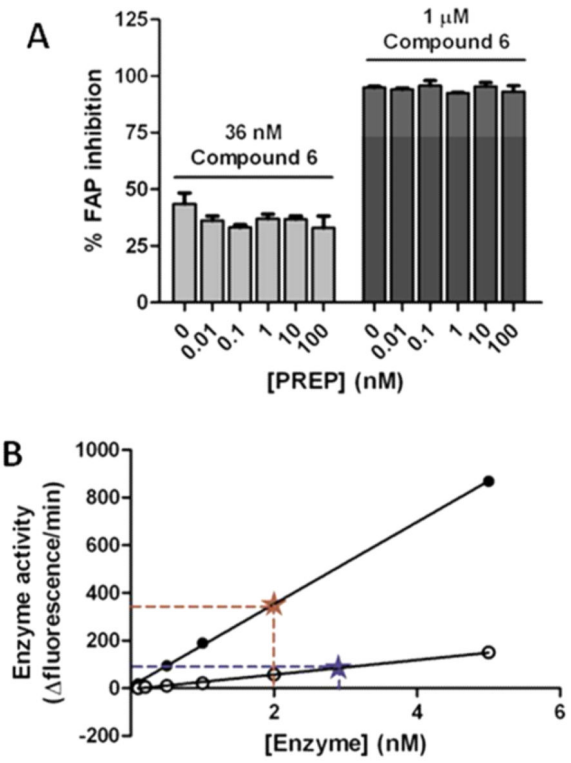

Figure 4.

Effect of the presence of PREP on FAP inhibition by **6**. (A) Recombinant FAP (1 nM) was mixed with varying concentrations of recombinant PREP and assayed for FAP inhibition by 36 nM (IC_{50}) or 1 μM **6**. (B) Standard curves were prepared for recombinant FAP (closed circles) and recombinant PREP (open circles) activity using 25 μM FAP specific substrate or Z-GP-AMC, respectively. FAP activity associated with 25 000 HEK-mFAP cells (red star) was measured using an FAP specific substrate and determined to be 2 nM. PREP activity associated with mock transfected HEK293 cells (blue star) was measured using Z-GP-AMC and determined to be 2.9 nM. This yields a cellular PREP to FAP ratio of 1:1.5. Error bars show the mean ± SEM.

NIH-PA Author Manuscript

NIH-PA Author Manuscript

NIH-PA Author Manuscript

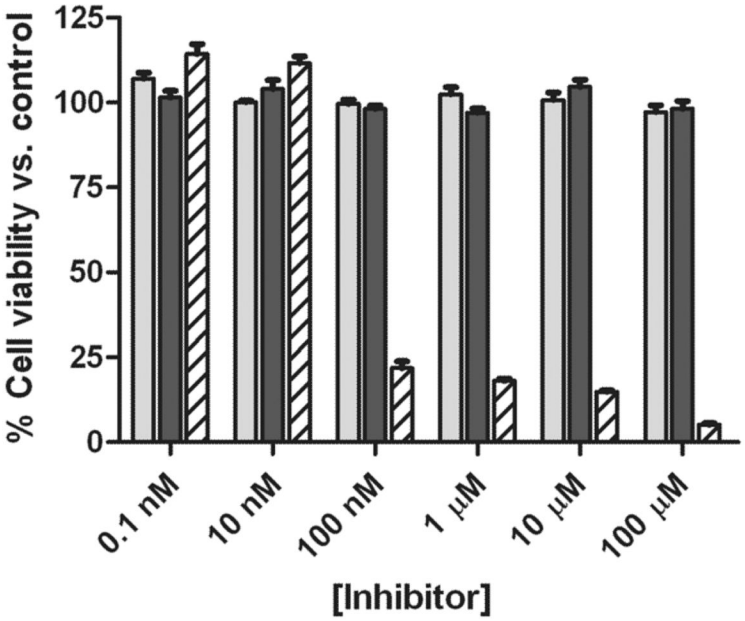

Figure 5.

Cytotoxicity of **6** in mFAP transfected HEK293 cells. Cells were treated with varying concentrations of 6 (light columns), **20** (dark columns), or bortezomib as a positive control (striped columns) for 48 h. Cytotoxicity was assessed using a CellTiter-Blue cell viability assay with calculation of percent cell viability based on vehicle treated control cells. Error bars show the mean ± SEM.

NIH-PA Author Manuscript

NIH-PA Author Manuscript

NIH-PA Author Manuscript

Table 1

FAP Selectivity of Compounds 1–6[a]

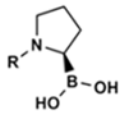

Compound	R	IC$_{50}$ (nM)					FAP selectivity
		DPPIV	DPP8	DPP9	FAP	PREP	
1	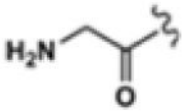	13 ± 2.1	180 ± 32	98 ± 20	52 ± 9.2	47,000 ± 45,000	900
2	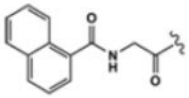	>100,000	1200 ± 300	420 ± 130	2.3 ± 0.4	1.8 ± 0.3	0.8
3	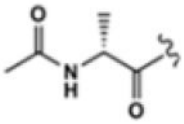	–	–	–	2900 ± 600	130 ± 19	0.04
4	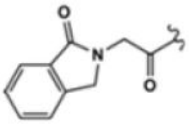	–	–	–	93 ± 11	7.2 ± 1.0	0.08
5	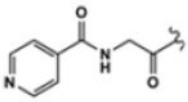	2800 ± 740	1,900 ± 260	1000 ± 570	0.47 ± 0.05	5.0 ± 0.7	11
6	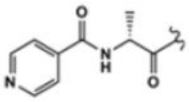	>100,000	5600 ± 1300	3400 ± 800	36 ± 4.8	13,000 ± 4300	360

[a]The FAP selectivity is equal to IC$_{50}$(PREP)/IC$_{50}$(FAP). IC$_{50}$ values are expressed with ±SEM.

NIH-PA Author Manuscript

NIH-PA Author Manuscript

NIH-PA Author Manuscript

Table 2

Comparison of FAP vs PREP against a Panel of N-Substituted D-Ala-boroPro-Based Inhibitors[a]

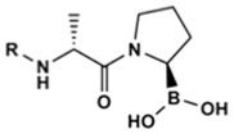

Compound	R	IC_{50} (nM)		FAP selectivity
		FAP	PREP	
7	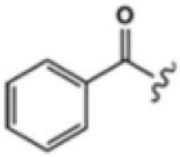	54 ± 2.9	1800 ± 240	33
8	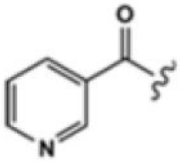	500 ± 95	91,000 ± 65,000	180
9	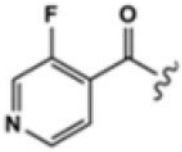	15 ± 0.9	1600 ± 190	110
10	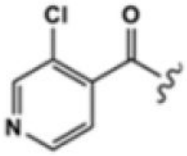	3.4 ± 0.4	640 ± 110	190
11	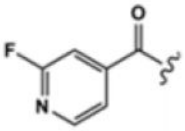	16 ± 2.9	2100 ± 260	130
12	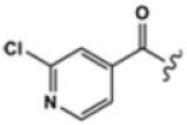	9.4 ± 1.1	1300 ± 200	140

[a]The FAP selectivity is equal to IC_{50}(PREP)/IC_{50}(FAP). IC_{50} values are expressed with ± SEM.

NIH-PA Author Manuscript

NIH-PA Author Manuscript

NIH-PA Author Manuscript

Table 3

Comparison of FAP vs PREP against a Panel of P_2 D-Amino Acid Substituted Inhibitors[a]

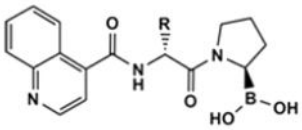

Compound	R	IC_{50}(nM) FAP	IC_{50}(nM) PREP	FAP selectivity
13	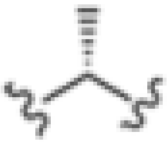	6.4 ± 1.4	1000 ± 250	160
14	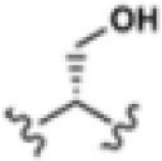	120 ± 27	440 ± 66	3.7
15	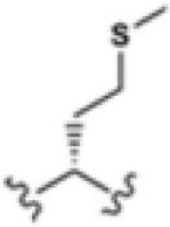	350 ± 81	26 ± 6.0	0.07
16		65 ± 19	96 ± 22	1.5
17		1300 ± 540	320 ± 92	0.25

NIH-PA Author Manuscript

NIH-PA Author Manuscript

NIH-PA Author Manuscript

Compound	R	IC_{50}(nM)		FAP selectivity
		FAP	PREP	
18	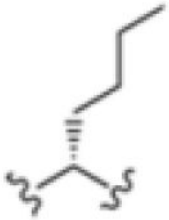	1100 ± 450	110 ± 27	0.1
19	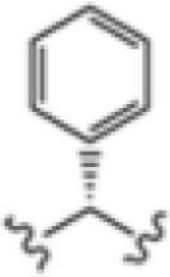	9300 ± 2,500	57 ± 14	001

[a]The FAP selectivity is equal to IC_{50}(PREP)/IC_{50}(FAP). IC_{50} values are expressed with ± SEM.

NIH-PA Author Manuscript

NIH-PA Author Manuscript

NIH-PA Author Manuscript

Table 4

PREP Selectivity of Compounds 20–22[a]

Compound	Structure	IC_{50} (HM)					PREP selectivity
		DPPIV	DPP8	DPP9	FAP	PREP	
20	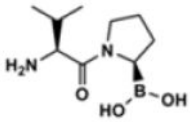	0.9 ± 0.1	5.5 ± 1.1	2.2 ± 0.4	12 ± 1.4	73 ± 22	0.16
21	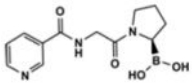	1800 ± 250	1700 ± 420	650 ± 170	1,1 ± 0.3	1.8 ± 0.2	0.61
22	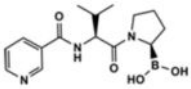	>100,000	>100,000	>100,000	>100,000	1.3 ± 0.2	>77,000

[a]The PREP selectivity is equal to IC_{50}(FAP)/IC_{50}(PREP). IC_{50} values are expressed with ± SEM.

NIH-PA Author Manuscript

NIH-PA Author Manuscript

NIH-PA Author Manuscript

Table 5

K_i Values for 6 and 22 against FAP and PREP[a]

	K_i (nM)		
inhibitor	**FAP**	**PREP**	**FAP selectivity**
6	9.0 ± 0.9	3100 ± 260	340
22		0.73 ± 0.15	

[a]Values are expressed with ± SEM.

NIH-PA Author Manuscript

NIH-PA Author Manuscript

NIH-PA Author Manuscript

Table 6

Chemical Building Blocks Utilized for the Synthesis of the N-Terminally Blocked X-boroPro Dipeptides

Compound	Structure	IUPAC	Addition Protocol
2	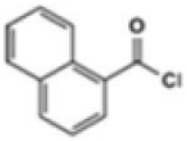	1 -naphthoyl chloride	IN NaOHin H_2O THF (1:4), 3N HCl
3	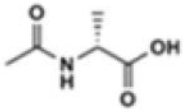	(2*R*)-2-(acetylamino)propanoic acid	HATU/DIPE in DMF
4	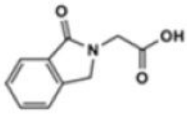	2-(1 -oxo-2.3 -dihydro -1 H-isoindol -2-yl)acetic acid	HATU/DIPEA in DMF
5 and **6**	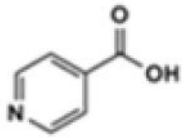	pyndme-4 -caiboxylic acid	HATU/DIPEA in DMF
7	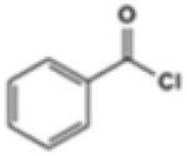	benzoyl chloride	DI PEA in CH_2Cl_2
8 and **22**	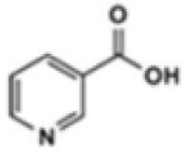	pyridine-3-carboxylic acid	HATU/DIPEA in DMF
9	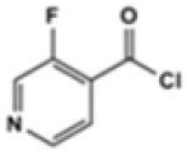	3 - fluoropyridine-4 -carboxy1ic acid	HATU/DIPEA in DMF

NIH-PA Author Manuscript

NIH-PA Author Manuscript

NIH-PA Author Manuscript

Compound	Structure	IUPAC	Addition Protocol
10	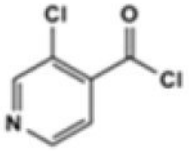	3-chloropyndine-4-carboxylic acid	HATU/DIPEA in DMF
11	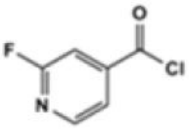	2-fluoropyndine-4 -cartoxylic acid	HATU/DIPEA in DMF
12	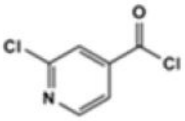	2-chloropyndme-4-carboxylic acid	HATU/DIPEA in DMF
13-19	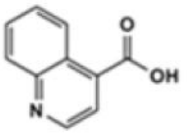	4-quinolinecarboxylic acid	HATU/DIPEA in DMF (**13-15,17,18**) EDC/HOBt in DMF (**16,19**)
21	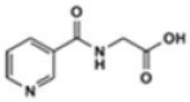	[(3-pyndrinylcarbonyl)amino) acetic acid	HATU/DIPEA in DMF